

REDUCING BERT PRE-TRAINING TIME FROM 3 DAYS TO 76 MINUTES

Yang You², Jing Li¹, Sashank Reddi¹, Jonathan Hseu¹, Sanjiv Kumar¹, Srinadh Bhojanapalli¹
Xiaodan Song¹, James Demmel², Cho-Jui Hsieh^{1,3}

Yang You was a student researcher at Google Brain. This project was done when he was at Google Brain.

Google¹, UC Berkeley², UCLA³

{youyang, demmel}@cs.berkeley.edu, {jingli, sashank, jhseu, sanjivk, bsrinadh, xiaodansong, chojui}@google.com

ABSTRACT

Training large deep neural networks on massive datasets is very challenging. One promising approach to tackle this issue is through the use of *large batch* stochastic optimization. However, our understanding of this approach in the context of deep learning is still very limited. Furthermore, the current approaches in this direction are heavily hand-tuned. To this end, we first study a general adaptation strategy to accelerate training of deep neural networks using large minibatches. Using this strategy, we develop a new layer-wise adaptive large batch optimization technique called LAMB. We also provide a formal convergence analysis of LAMB as well as the previous published layerwise optimizer LARS, showing convergence to a stationary point in general nonconvex settings. Our empirical results demonstrate the superior performance of LAMB for BERT and ResNet-50 training. In particular, for BERT training, our optimization technique enables use of very large batches sizes of 32868; thereby, requiring just 8599 iterations to train (as opposed to 1 million iterations in the original paper). By increasing the batch size to the memory limit of a TPUv3 pod, BERT training time can be reduced from 3 days to 76 minutes (Table 1). Finally, we also demonstrate that LAMB outperforms previous large-batch training algorithms for ResNet-50 on ImageNet; obtaining state-of-the-art performance in just a few minutes.

1 INTRODUCTION

With the advent of large scale datasets, training large deep neural networks, even using computationally efficient optimization methods like Stochastic gradient descent (SGD), has become particularly challenging. For instance, training state-of-the-art deep learning models like BERT and ResNet-50 takes 3 days on 16 TPUv3 chips and 29 hours on 8 Tesla P100 gpus respectively. Thus, there is a growing interest to develop optimization solutions to tackle this critical issue. The goal of this paper is to investigate and develop optimization techniques to accelerate training large deep neural networks, mostly focusing on approaches based on variants of SGD.

Methods based on SGD iteratively update the parameters of the model by moving them in a scaled (negative) direction of the gradient calculated on a minibatch. However, SGD’s scalability is limited by its inherent sequential nature. Owing to this limitation, traditional approaches to improve SGD training time in the context of deep learning largely resort to distributed asynchronous setup (Dean et al., 2012; Recht et al., 2011). However, the implicit staleness introduced due to the asynchrony limits the parallelization of the approach; often leading to degraded performance. The feasibility of computing gradient on large minibatches in parallel due to recent advances has seen the resurgence of simply using synchronous SGD with large minibatches as an alternative to asynchronous SGD.

Synchronous SGD on large minibatches benefits from reduced variance of the stochastic gradients used in SGD. This allows one to use much larger learning rates in SGD, typically of the order square root of the minibatch size. Surprisingly, recent works have demonstrated that up to certain minibatch sizes, linear scaling of the learning with minibatch size can be used to further speed up the training. These works also elucidate two interesting aspects to enable the use of linear scaling in large batch synchronous SGD: (i) linear scaling of learning rate is harmful during the initial phase; thus, a hand-tuned warmup strategy of slowing increasing the learning rate needs to be used initially, and

(ii) linear scaling of learning rate can be detrimental beyond a certain batch size. Using these tricks, Goyal et al. (2017) was able to drastically reduce the training time of ResNet-50 model from 29 hours to 1 hour using a batch size of 8192. While these works demonstrate the feasibility of this strategy for reducing the wall time for training large deep neural networks, they also highlight the need for an adaptive learning rate mechanism for large batch learning.

Layerwise adaptive learning rates have been recently studied for this problem. The most successful in this line of research is the LARS algorithm (You et al., 2017), which was initially proposed for training RESNET. Using LARS, ResNet-50 can be trained on ImageNet in just a few minutes! However, a theoretical understanding of the adaptation employed in LARS is largely missing.

Contributions. In the light of this background, we state the following main contributions of the paper.

- Inspired by LARS, we investigate a general adaptation strategy specially catered to large batch learning and provide intuition for the strategy.
- Based on the adaptation strategy, we develop a new optimization algorithm (LAMB) for achieving adaptivity of learning rate in SGD. Furthermore, we provide convergence analysis for both LARS and LAMB to achieve a stationary point in nonconvex settings. We highlight the benefits of using these methods for large batch settings.
- We demonstrate the strong empirical performance of LAMB across several challenging tasks. Using LAMB we scale the batch size in training BERT to more than 32k without degrading the performance; thereby, cutting the time down from 3 days to 76 minutes. Ours is the first work to reduce BERT training wall time to less than couple of hours.
- We also demonstrate the efficiency of LAMB for training state-of-the-art image classification models like RESNET. To the best of our knowledge, ours is first adaptive solver that can achieve state-of-the-art accuracy for RESNET-50 as adaptive solvers like Adam fail to obtain the accuracy of defacto SGD with momentum for these tasks.

1.1 RELATED WORK

The literature on optimization for machine learning is vast and hence, we restrict our attention to the works on large batch settings that are most relevant to our paper. Earlier works on large batch optimization for machine learning mostly focused on convex models. It is known that for general stochastic convex objective functions, the convergence of SGD with minibatch b is $O(1/\sqrt{bT} + 1/T)$. If a more complex optimization problem is solved in each iteration, the convergence rate can be improved to $O(1/\sqrt{bT})$, which improves when batch size b is large. Similar results can be shown for nonconvex settings wherein using larger minibatches improves the convergence to stationary points; albeit at the cost of extra computation. However, several important concerns were raised with respect to generalization and computational performance in large batch nonconvex settings. It was observed that training with extremely large batch was difficult (Keskar et al., 2016; Hoffer et al., 2017). The researchers needed to carefully tune training hyper-parameters, like learning rate and momentum, to avoid losing test accuracy (Goyal et al., 2017; Li, 2017; You et al., 2018; Shallue et al., 2018).

Krizhevsky (2014) introduced some practical schemes for training with large batches. One important rule is to increase the LR (learning rate) by \sqrt{b} when batch size is scaled by b since the variance of the gradient estimation decreases by a factor of b . In practice, (Krizhevsky, 2014) found that linear scaling works better upto certain batch sizes. To avoid optimization instability due to high learning rate, Goyal et al. (2017) proposed to use a highly hand-tuned learning rate warm-up strategy which starts with a small LR and then gradually increases the LR to a larger value. After warm-up period (usually a few epochs) one switches to the regular LR policy (multi-steps, exponential or polynomial decay etc). Using LR warm-up and linear scaling, Goyal et al. (2017) managed to train RESNET-50 with batch size 8192 without loss in test accuracy. However, empirical study (Shallue et al., 2018) shows that learning rate scaling heuristics with the batch size do not hold across all problems or across all batch sizes.

More recently, to reduce hand-tuning of hyperparameters, adaptive learning rates for large batch training garnered significant interest. Several recent works successfully scaled the batch size to large values using adaptive learning rates without degrading the performance, thereby, finishing RESNET-50 training on ImageNet in a few minutes (You et al., 2018; Iandola et al., 2016; Codreanu et al., 2017; Akiba et al., 2017; Jia et al., 2018; Smith et al., 2017; Martens & Grosse, 2015; Devarakonda

et al., 2017; Mikami et al., 2018; Osawa et al., 2018; You et al., 2019). To the best of our knowledge, the fastest training result for RESNET-50 on ImageNet is due to (Ying et al., 2018), who achieve 76+% top-1 accuracy. By using the LARS optimizer and scaling the batch size to 32K on a TPUv3 Pod, Ying et al. (2018) was able to train RESNET-50 on ImageNet in 2.2 minutes.

2 PRELIMINARIES

Notation For any vector $x_t \in \mathbb{R}^d$, either $x_{t,j}$ or $[x_t]_j$ are used to denote its j^{th} coordinate where $j \in [d]$. Let \mathbb{I} be the $d \times d$ identity matrix, and let $\mathbb{I} = [\mathbb{I}_1, \mathbb{I}_2, \dots, \mathbb{I}_h]$ be its decomposition into column submatrices $\mathbb{I}_i = d \times d_h$. For $x \in \mathbb{R}^d$, let $x^{(i)}$ be the block of variables corresponding to the columns of \mathbb{I}_i i.e., $x^{(i)} = \mathbb{I}_i^\top x \in \mathbb{R}^{d_i}$ for $i = \{1, 2, \dots, h\}$. Note that any vector $x \in \mathbb{R}^d$ can be written, uniquely, as $x = \mathbb{I}_i x^{(i)}$. We will use these notations to denote network parameters in different layers. For any function $f : \mathbb{R}^d \rightarrow \mathbb{R}$, we use $\nabla_i f(x)$ to denote the gradient with respect to $x^{(i)}$. We use $\|\cdot\|$ and $\|\cdot\|_1$ to denote l_2 -norm and l_1 -norm of a vector respectively.

We now formally state the problem setup. In this paper, we study nonconvex stochastic optimization problems of the form

$$\min_{x \in \mathbb{R}^d} f(x) := \mathbb{E}_{s \sim \mathbb{P}}[\ell(x, s)] + \frac{\lambda}{2} \|x\|^2, \quad (1)$$

where ℓ is a smooth (possibly nonconvex) function and \mathbb{P} is a probability distribution on the domain $\mathcal{S} \subset \mathbb{R}^k$. Here, x corresponds to model parameters, ℓ is the loss function and \mathbb{P} is an unknown data distribution.

We assume function $\ell(x)$ is L_i -smooth with respect to $x^{(i)}$, i.e., there exists a constant L_i such that

$$\|\nabla_i \ell(x, s) - \nabla_i \ell(y, s)\| \leq L_i \|x^{(i)} - y^{(i)}\|, \quad \forall x, y \in \mathbb{R}^d, \text{ and } s \in \mathcal{S}, \quad (2)$$

for all $i \in [h]$. We use $L = (L_1, \dots, L_h)^\top$ to denote the h -dimensional vector of Lipschitz constants. Also, we use L_∞ to denote $\max_i L_i$. The following bound is assumed on the variance in stochastic gradients: $\mathbb{E} \|\nabla_i \ell(x, s) - \nabla_i f(x)\|^2 \leq \sigma_i^2$ for all $x \in \mathbb{R}^d$ and $i \in [h]$. Furthermore, we also assume $\mathbb{E} \|\nabla \ell(x, s)\|_i - \|\nabla f(x)\|_i\|^2 \leq \tilde{\sigma}_i^2$ for all $x \in \mathbb{R}^d$ and $i \in [d]$. We use $\sigma = (\sigma_1, \dots, \sigma_h)^\top$ and $\tilde{\sigma} = (\tilde{\sigma}_1, \dots, \tilde{\sigma}_d)^\top$ to denote the vectors of standard deviations of stochastic gradient per layer and per dimension respectively. Finally, we assume that the gradients are bounded i.e., $\|\nabla \ell(x, s)\|_j \leq G$ for all $i \in [d]$, $x \in \mathbb{R}^d$ and $s \in \mathcal{S}$. Note that such assumptions are typical in the analysis of stochastic first-order methods (cf. (Ghadimi & Lan, 2013a; Ghadimi et al., 2014)).

Stochastic gradient descent (SGD) is one of the simplest first-order algorithms for solving equation 1. The update at the t^{th} iteration of SGD is of the following form:

$$x_{t+1} = x_t - \eta_t \frac{1}{|\mathcal{S}_t|} \sum_{s_t \in \mathcal{S}_t} \nabla \ell(x_t, s_t) + \lambda x_t, \quad (\text{SGD})$$

where \mathcal{S}_t is set of b random samples drawn from the distribution \mathbb{P} . However, tuning the learning rate η_t in SGD, especially in large batch settings, is difficult. In the next section, we discuss algorithms to circumvent this issue. The following is a well-known result for SGD in large batch setting.

Theorem 1 ((Ghadimi & Lan, 2013b)). *With large batch $b = T$ and using appropriate learning rate, we have the following for the iterates of SGD:*

$$\mathbb{E} [\|\nabla f(x_a)\|^2] \leq O \left(\frac{(f(x_1) - f(x^*))L_\infty}{T} + \frac{\|\sigma\|^2}{T} \right).$$

where x^* is an optimal solution to the problem in equation 1 and x_a is an iterate uniformly randomly chosen from $\{x_1, \dots, x_T\}$.

3 ALGORITHMS

In this section, we first discuss a general strategy to adapt the learning rate in large batch settings. Using this strategy, we discuss two specific algorithms in the later part of the section. Since our

primary focus is on training deep neural networks, our discussion is centered around training a h -layer neural network.

General Strategy. Suppose we use an iterative algorithm \mathcal{A} in the small batch setting with the following layerwise update rule:

$$x_{t+1} = x_t + \eta_t u_t,$$

where u_t is the update made by \mathcal{A} at time step t . We propose the following two changes to the update for large batch settings:

1. The update is normalized to unit l_2 -norm. This is ensured by modifying the update to the form $u_t/\|u_t\|$. Throughout this paper, such a normalization is done layerwise i.e., the update for each layer is ensured to be unit l_2 -norm.
2. The learning rate is scaled by $\phi(\|x_t\|)$ for some function $\phi : \mathbb{R}^+ \rightarrow \mathbb{R}^+$. Similar to the normalization, such a scaling is done layerwise.

Suppose algorithm \mathcal{A} is simple SGD, then the modification results in the following update rule:

$$x_{t+1}^{(i)} = x_t^{(i)} - \eta_t \frac{\phi(\|x_t^{(i)}\|)}{\|g_t^{(i)}\|} g_t^{(i)}, \quad (3)$$

for all layers $i \in [h]$ and where $x_t^{(i)}$ and $g_t^{(i)}$ are the parameters and the gradients of the i^{th} layer at time step t . The normalization modification is similar to one typically used in normalized gradient descent except that it is done layerwise. Note that the modification leads to biased gradient update; however, in large-batch settings, it can be shown that this bias is small. It is intuitive that such a normalization provides robustness to exploding gradients (where the gradient can be arbitrarily large) and plateaus (where the gradient can be arbitrarily small). Normalization of this form essentially ignores the size of the gradient and is particularly useful in large batch settings where the direction of the gradient is largely preserved.

The scaling term involving ϕ ensures that the norm of the update is of the same order as that of the parameter. We found that this typically ensures faster convergence in deep neural networks. In practice, we observed that a simple function of $\phi(z) = \min\{\max\{z, \gamma_l\}, \gamma_u\}$ works well. It is instructive to consider the case where $\phi(z) = z$. In this scenario, the overall change in the learning rate is $\frac{\|x_t^{(i)}\|}{\|g_t^{(i)}\|}$, which can also be interpreted as an estimate on the inverse of Lipschitz constant of the gradient (see equation 2).

We now discuss different instantiations of the strategy discussed above. In particular, we focus on two algorithms: LARS (3.1) and the proposed method, LAMB (3.2).

3.1 LARS ALGORITHM

The first instantiation of the general strategy is LARS algorithm (You et al., 2017), which is obtained by using momentum optimizer as algorithm \mathcal{A} in the framework. LARS was earlier proposed for large batch learning for RESNET on ImageNet. In general, it is observed that the using (heavy-ball) momentum, one can reduce the variance in the stochastic gradients at the cost of little bias. The pseudocode for LARS is provide in Algorithm 1.

We now provide convergence analysis for LARS in general nonconvex setting stated in this paper. For the sake of simplicity, we analyze the case where $\beta_1 = 0$ and $\lambda = 0$ in Algorithm 1. However, our analysis should extend to the general case as well. We will defer discussion about the convergence rate to the end of the section.

Theorem 2. Let $\eta_t = \eta = \sqrt{\frac{2(f(x_1) - f(x^*))}{\alpha_u^2 \|L\|_1 T}}$ for all $t \in [T]$, $b = T$, $\alpha_l \leq \phi(v) \leq \alpha_u$ for all $v > 0$ where $\alpha_l, \alpha_u > 0$. Then for x_t generated using LARS (Algorithm 1), we have the following bound

$$\left(\mathbb{E} \left[\sum_{i=1}^h \|\nabla_i f(x_a)\| \right] \right)^2 \leq O \left(\frac{(f(x_1) - f(x^*)) \|L\|_1}{T} + \frac{\|\sigma\|_1^2}{T} \right),$$

where x^* is an optimal solution to the problem in equation 1 and x_a is an iterate uniformly randomly chosen from $\{x_1, \dots, x_T\}$.

Algorithm 1 LARS

Input: $x_1 \in \mathbb{R}^d$, learning rate $\{\eta_t\}_{t=1}^T$, parameter $0 < \beta_1 < 1$, scaling function ϕ , $\epsilon > 0$
Set $m_0 = 0$
for $t = 1$ **to** T **do**
 Draw b samples S_t from \mathbb{P}
 Compute $g_t = \frac{1}{|S_t|} \sum_{s_t \in S_t} \nabla \ell(x_t, s_t)$
 $m_t = \beta_1 m_{t-1} + (1 - \beta_1)(g_t + \lambda x_t)$
 $x_{t+1}^{(i)} = x_t^{(i)} - \eta_t \frac{\phi(\|x_t^{(i)}\|)}{\|m_t^{(i)}\|} m_t^{(i)}$ for all $i \in [h]$
end for

Algorithm 2 LAMB

Input: $x_1 \in \mathbb{R}^d$, learning rate $\{\eta_t\}_{t=1}^T$, parameters $0 < \beta_1, \beta_2 < 1$, scaling function ϕ , $\epsilon > 0$
Set $m_0 = 0, v_0 = 0$
for $t = 1$ **to** T **do**
 Draw b samples S_t from \mathbb{P} .
 Compute $g_t = \frac{1}{|S_t|} \sum_{s_t \in S_t} \nabla \ell(x_t, s_t)$.
 $m_t = \beta_1 m_{t-1} + (1 - \beta_1)g_t$
 $v_t = \beta_2 v_{t-1} + (1 - \beta_2)g_t^2$
 Compute ratio $r_t = \frac{m_t}{\sqrt{v_t + \epsilon}}$
 $x_{t+1}^{(i)} = x_t^{(i)} - \eta_t \frac{\phi(\|x_t^{(i)}\|)}{\|r_t^{(i)} + \lambda x_t^{(i)}\|} (r_t^{(i)} + \lambda x_t)$
end for

3.2 LAMB ALGORITHM

The second instantiation of the general strategy is obtained by using ADAM optimizer as algorithm \mathcal{A} . ADAM optimizer is popular in deep learning community and has shown to have good performance for training state-of-the-art language models like BERT. Unlike LARS, the adaptivity of LAMB is two-fold: (i) per dimension normalization with respect to the square root of the second moment used in ADAM and (ii) layerwise normalization obtained due to layerwise adaptivity. The pseudocode for LAMB is provided in Algorithm 2. When $\beta_1 = 0$ and $\beta_2 = 0$, the algorithm reduces to be Sign SGD where the learning rate is scaled by square root of the layer dimension (Bernstein et al., 2018).

The following result provides convergence rate for LAMB in general nonconvex settings. Similar to the previous case, we focus on the setting where $\beta_1 = 0$ and $\lambda = 0$. As before, our analysis extends to the general case; however, the calculations become messy.

Theorem 3. Let $\eta_t = \eta = \sqrt{\frac{2(f(x_1) - f(x^*))}{\alpha_u^2 \|L\|_1 T}}$ for all $t \in [T]$, $b = T$, $d_i = d/h$ for all $i \in [h]$, and $\alpha_l \leq \phi(v) \leq \alpha_u$ for all $v > 0$ where $\alpha_l, \alpha_u > 0$. Then for x_t generated using LAMB (Algorithm 2), we have the following bounds:

1. When $\beta_2 = 0$, we have

$$(\mathbb{E}[\|\nabla f(x_a)\|_1])^2 \leq O\left(\frac{d}{h} \times \left[\frac{(f(x_1) - f(x^*))\|L\|_1}{T} + \frac{\|\tilde{\sigma}\|_1^2}{T}\right]\right),$$

2. When $\beta_2 > 0$, we have

$$\mathbb{E}[\|\nabla f(x_a)\|^2] \leq O\left(\sqrt{\frac{G^2 d}{h(1 - \beta_2)}} \times \left[\sqrt{\frac{2(f(x_1) - f(x^*))\|L\|_1}{T}} + \frac{\|\tilde{\sigma}\|_1}{\sqrt{T}}\right]\right),$$

where x^* is an optimal solution to the problem in equation 1 and x_a is an iterate uniformly randomly chosen from $\{x_1, \dots, x_T\}$.

Discussion on convergence rates. We first start our discussion with the comparison of convergence rate of LARS with that of SGD (Theorem 1). The convergence rates of LARS and SGD differ in two ways: (1) the convergence criterion is $(\mathbb{E}[\sum_{i=1}^h \|\nabla_i f\|])^2$ as opposed to $\mathbb{E}[\|\nabla f\|^2]$ in SGD and (2) the dependence on L and σ in the convergence rate. Briefly, the convergence rate of LARS is better than SGD when the gradient is denser than curvature and stochasticity. This convergence rate comparison is similar in spirit to the one obtained in (Bernstein et al., 2018). A more quantitative comparison is provided in Section C of the Appendix. The comparison of LAMB (with $\beta_2 = 0$) with SGD is along similar lines. We obtain slightly worse rates for the case where $\beta_2 > 0$; although, we believe that its behavior should be better than the case $\beta_2 = 0$. We leave this investigation to future work.

4 EXPERIMENTS

We now present empirical results comparing LAMB with existing optimizers on two important large batch training tasks: BERT and ResNet-50 training. In the later part of the section, we also show the performance of LAMB on a few small tasks involving CIFAR and MNIST datasets.

Experimental Setup. To demonstrate its robustness, we use very minimal hyperparameter tuning for the LAMB optimizer. Thus, it is possible to achieve better results by further tuning the hyperparameters. The parameters β_1 and β_2 in Algorithm 2 are set to 0.9 and 0.999 respectively in all our experiments. We only tune the learning rate. We use a polynomial decay with the power of 1.0 ($n_t = n_0 \times (1 - t/T)$ in Algorithm 2), which is the same as the BERT baseline. This setting works for all the other applications in this paper. Furthermore, for BERT and ResNet-50 training, we did not tune the hyperparameters of LAMB while increasing the batch size. We use the square root of LR scaling rule Krizhevsky (2014) to automatically adjust learning rate and linear-epoch warmup scheduling You et al. (2019). We use TPUv3 in all the experiments. A TPUv3 Pod has 1024 chips and can provide more than 100 petaflops performance for mixed precision computing. Due to space constraints, several experimental details are relegated to the Appendix.

To make sure we are comparing with solid baselines, we use grid search to tune the hyper-parameters for ADAM, ADAGRAD, ADAMW (ADAM with weight decay), and LARS. We also tune weight decay for ADAMW. All the hyperparameter tuning settings are reported in the Appendix.

4.1 BERT TRAINING

We first discuss empirical results for speeding up BERT pre-training. For this experiment, we use the same dataset as (Devlin et al., 2018), which is a concatenation of Wikipedia and BooksCorpus with 2.5B and 800M words respectively. We specifically focus on the SQuAD task in this paper. Stanford Question Answering Dataset (SQuAD) is a reading comprehension dataset which contains questions posed by crowdworkers on a set of Wikipedia articles, the answer to which is a segment of text from the provided reading passage¹. The F1 score on SQuAD-v1 is used as the accuracy metric in our experiments. All our comparisons are with respect to the baseline BERT model in (Devlin et al., 2018). To train BERT, Devlin et al. (2018) first train the model for 900k iterations using sequence length of 128 and then switch to sequence length of 512 for the last 100k iterations. This results in a training time of around 3 days on 16 TPUv3 chips. The baseline BERT model² achieves a F1 score of 90.395. To ensure a fair comparison, we follow the same SQuAD fine-tune procedure of (Devlin et al., 2018) without modifying any configuration (including number of epochs and hyperparameters). As noted earlier, we could get even better results by changing the fine-tune configuration. For instance, by just slightly changing the learning rate in the fine-tune stage, we can obtain a higher F1 score of 91.688 for the batch size of 16K using LAMB. We report a F1 score of 91.345 in Table 1, which is the score obtained for the untuned version. Below we describe two different training choices for training BERT using LAMB and discuss the corresponding speedups.

Regular Training using LAMB For the first choice, we maintain the same training procedure as the baseline except for changing the pre-training optimizer to LAMB. We run with the same number of epochs as the baseline but with batch size scaled from 512 to 32K. The choice of 32K batch size (with sequence length 512) is mainly due to memory limits of TPU Pod. Our results are shown in Table 1. By using the LAMB optimizer, we are able to achieve a F1 score of 91.460 in 15625 iterations for a batch size of 32768 (14063 iterations for sequence length 128 and 1562 iterations for sequence length 512). With 32K batch size, we reduce BERT pre-training time from 3 days to around 100 minutes. The loss curves of BERT training by LAMB for different batch sizes are shown in Figure 1. We observe that the loss curves are almost identical to each other, which means our optimizer scales well with the batch size. We achieved 76.7% scaling efficiency (49.1 times speedup by 64 times computational resources). We consider 76.7% scaling efficiency is great because we use the synchronous data-parallelism for distributed training on the TPU Pod. There is a communication overhead coming from transferring of the gradients over the interconnect. The gradients have the same size of the trained models. For ImageNet training with RESNET-50, researchers are able to achieve 90% scaling efficiency because ResNet-50 has much fewer parameters than BERT (25 million versus 300 million).

¹<https://rajpurkar.github.io/SQuAD-explorer/>

²Pre-trained BERT model can be downloaded from <https://github.com/google-research/bert>

Table 1: We use the F1 score on SQuAD-v1 as the accuracy metric. The baseline F1 score is the score obtained by the pre-trained model (BERT-Large) provided on BERT’s public repository (as of February 1st, 2019). We use TPUv3s in our experiments. We use the same setting as the baseline: the first 9/10 of the total epochs used a sequence length of 128 and the last 1/10 of the total epochs used a sequence length of 512. All the experiments run the same number of epochs. Dev set means the test data. It is worth noting that we can achieve better results by manually tuning the hyperparameters.

Solver	batch size	steps	F1 score on dev set	TPUs	Time
Baseline	512	1000k	90.395	16	81.4h
LAMB	512	1000k	91.752	16	82.8h
LAMB	1k	500k	91.761	32	43.2h
LAMB	2k	250k	91.946	64	21.4h
LAMB	4k	125k	91.137	128	693.6m
LAMB	8k	62500	91.263	256	390.5m
LAMB	16k	31250	91.345	512	200.0m
LAMB	32k	15625	91.475	1024	101.2m
LAMB	64k/32k	8599	90.584	1024	76.19m

Table 2: ADAMW stops scaling at the batch size of 16K. The target F1 score is 90.5. LAMB achieves a F1 score of 91.345.

Solver	batch size	warmup steps	LR	last step information	F1 score on dev set
ADAMW	16K	0.05×31250	0.0001	loss=8.04471, step=28126	diverged
ADAMW	16K	0.05×31250	0.0002	loss=7.89673, step=28126	diverged
ADAMW	16K	0.05×31250	0.0003	loss=8.35102, step=28126	diverged
ADAMW	16K	0.10×31250	0.0001	loss=2.01419, step=31250	86.034
ADAMW	16K	0.10×31250	0.0002	loss=1.04689, step=31250	88.540
ADAMW	16K	0.10×31250	0.0003	loss=8.05845, step=20000	diverged
ADAMW	16K	0.20×31250	0.0001	loss=1.53706, step=31250	85.231
ADAMW	16K	0.20×31250	0.0002	loss=1.15500, step=31250	88.110
ADAMW	16K	0.20×31250	0.0003	loss=1.48798, step=31250	85.653

Mixed-Batch Training using LAMB To obtain further improvements, we use the following training procedure with LAMB. Recall that BERT pre-training involves two stages: the first 9/10 of the total epochs use a sequence length of 128, while the last 1/10 of the total epochs use a sequence length of 512. For the second stage, which involves a larger sequence length, due to memory limits, a maximum batch size of only 32768 can be used on a TPUv3 Pod. However, we can potentially use a larger batch size for the first stage because of smaller sequence length. In particular, the batch size can be increased to 131072 for the first stage. However, we did not observe any speedup by increasing the batch size from 65536 to 131072 for the first stage, thus, we restrict the batch size to 65536 for this stage. By using this strategy, we are able to make full utilization of the hardware resources throughout the training procedure. Increasing the batch size is able to warm-up and stabilize the optimization process [Smith et al. \(2017\)](#), but decreasing the batch size brings chaos to the optimization process and can cause divergence. In our experiments, we found a technique that is useful to stabilize the second stage optimization. Because we switched to a different optimization problem, it is necessary to re-warm-up the optimization. Instead of decaying the learning rate at the second stage, we ramp up the learning rate from zero again in the second stage (re-warm-up). As with the first stage, we decay the learning rate after the re-warm-up phase. With these changes, we only need 8599 iterations and can finish BERT training in around 76 minutes. Figure 2 shows that we can achieve 76.8% scaling efficiency by scaling the batch size (49.1 times speedup by 64 times computational resources) and 101.8% scaling efficiency with mixed-batch (65.2 times speedup by 64 times computational resources)

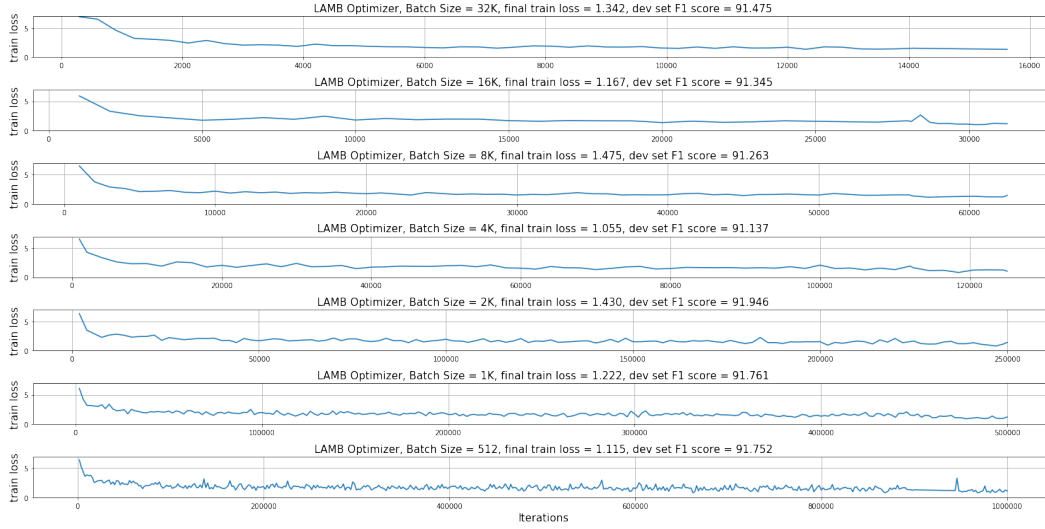


Figure 1: This figure shows the training loss curve of LAMB optimizer. We just want to use this figure to show that LAMB can make the training converge smoothly. Even if we scale the batch size to the extremely large cases, the loss curves are almost identical to each other.

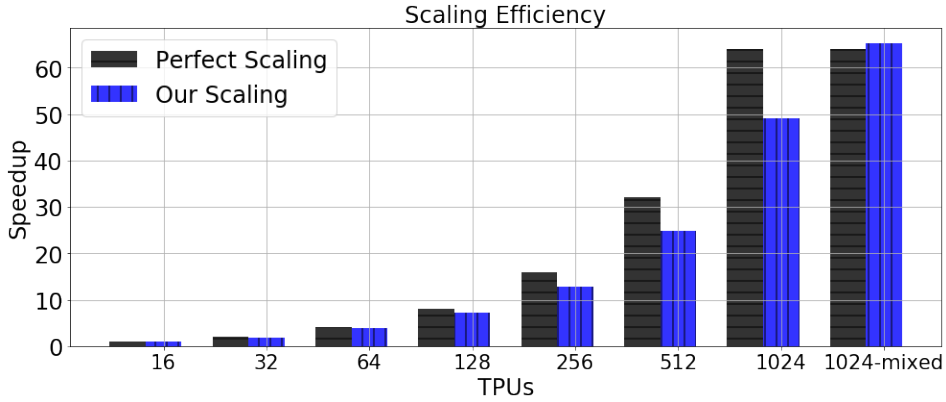


Figure 2: We achieve 76.8% scaling efficiency (49 times speedup by 64 times computational resources) and 101.8% scaling efficiency with a mixed, scaled batch size (65.2 times speedup by 64 times computational resources). 1024-mixed means the mixed-batch training on 1024 TPUs.

Comparison with ADAMW and LARS. To ensure that our approach is compared to a solid baseline for the BERT pre-training, we tried three different strategies for tuning ADAMW: (1) ADAMW with default hyperparameters (see (Devlin et al., 2018)) (2) ADAMW with the same hyperparameters as LAMB, and (3) ADAMW with tuned hyperparameters. ADAMW stops scaling beyond batch size of 16K because it is not able to achieve the target F1 score (88.1 vs 90.4). Table 2 shows some of the tuning information. For 64K/32K mixed-batch training, even after extensive tuning of the hyperparameters, we fail to get any reasonable result with ADAMW optimizer. We conclude that ADAMW does not work well in large-batch BERT pre-training or is at least hard to tune. We also observe that LAMB performs better than LARS for all batch sizes (see Table 3).

4.2 IMAGENET TRAINING WITH RESNET-50.

ImageNet training with ResNet-50 is an industry standard metric that is being used in MLPerf³. A correct implementation can get 76.3% top-1 accuracy in 90 epochs (Goyal et al., 2017). All

³<https://mlperf.org/>

Table 3: LAMB achieves a higher performance (F1 score) than LARS for all the batch sizes. The baseline achieves a F1 score of 90.390. Thus, LARS stops scaling at the batch size of 16K.

Batch Size	512	1K	2K	4K	8K	16K	32K
LARS	90.717	90.369	90.748	90.537	90.548	89.589	diverge
LAMB	91.752	91.761	91.946	91.137	91.263	91.345	91.475

the successful implementations are based on Momentum optimizer (He et al., 2016; Goyal et al., 2017) or LARS optimizer (Ying et al., 2018; Jia et al., 2018; Mikami et al., 2018; You et al., 2018). We do not find any paper or article reporting a state-of-the-art accuracy achieved by ADAM, ADAGRAD, or ADAMW optimizer. In our experiments, even with comprehensive hyper-parameter tuning, ADAGRAD/ADAM/ADAMW (with batch size 16K) only achieves 55.38%/66.04%/67.27% top-1 accuracy. After adding learning rate scheme of Goyal et al. (2017), the top-1 accuracy of ADAGRAD/ADAM/ADAMW was improved to 72.0%/73.48%/73.07%. However, they are still much lower than 76.3%. The details of the tuning information are in the appendix. Table 4 shows that LAMB can achieve the target accuracy. Beyond a batch size of 8K, LAMB’s accuracy is higher than the momentum. LAMB’s accuracy is also slightly better than LARS. At a batch size of 32K, LAMB achieves 76.4% top-1 accuracy while LARS achieves 76.3%. At a batch size of 2K, LAMB is able to achieve 77.11% top-1 accuracy while LARS achieves 76.6%.

Table 4: Top-1 validation accuracy of ImageNet/ResNet-50 training at the batch size of 16K. The performance of momentum was reported by (Goyal et al., 2017). ADAM+ means adding the learning rate scheme of Goyal et al. (2017) to ADAM: (1) 5-epoch warmup to stabilize the initial stage; and (2) multiply the learning rate by 0.1 at 30th, 60th, and 80th epoch. The target accuracy is around 0.763 (Goyal et al., 2017). All the adaptive solvers were comprehensively tuned. The tuning information was in the appendix.

Optimizer	ADAGRAD/ADAGRAD+	ADAM/ADAM+	ADAMW/ADAMW+	momentum	LAMB
Accuracy	0.5538/0.7201	0.6604/0.7348	0.6727/0.7307	0.7520	0.7666

4.3 HYPERPARAMETERS FOR SCALING THE BATCH SIZE

For BERT and ImageNet training, we did not tune the hyperparameters of LAMB optimizer when increasing the batch size. We use the square root LR scaling rule (Krizhevsky, 2014) to automatically adjust learning rate and linear-epoch warmup scheduling (You et al., 2019). The details can be found in Tables 5 and 6

Table 5: Untuned LAMB for BERT pre-training across different batch sizes. We can just use square root LR scaling (Krizhevsky, 2014) and linear-epoch warmup (You et al., 2019). For example, Batch Size 32K needs to finish 15625 iterations. It uses $0.2 \times 15625 = 3125$ iterations for learning rate warmup. BERT’s baseline achieved a F1 score of 90.395. We can achieve better accuracy for 32K if we manually tune the hyperparameters.

Batch Size	512	1K	2K	4K	8K	16K	32K
Learning Rate	$\frac{5}{2^{3.0} \times 10^3}$	$\frac{5}{2^{2.5} \times 10^3}$	$\frac{5}{2^{2.0} \times 10^3}$	$\frac{5}{2^{1.5} \times 10^3}$	$\frac{5}{2^{1.0} \times 10^3}$	$\frac{5}{2^{0.5} \times 10^3}$	$\frac{5}{2^{0.0} \times 10^3}$
Warmup Ratio	$\frac{1}{320}$	$\frac{1}{160}$	$\frac{1}{80}$	$\frac{1}{40}$	$\frac{1}{20}$	$\frac{1}{10}$	$\frac{1}{5}$
F1 score	91.752	91.761	91.946	91.137	91.263	91.345	91.475

4.4 REGULAR BATCH SIZES FOR SMALL DATASETS: MNIST AND CIFAR-10.

According to DAWNBench, DavidNet (a custom 9-layer Residual ConvNet) is the fastest model for CIFAR-10 dataset (as of April 1st, 2019)⁴. The baseline uses the momentum optimizer. Table 7 shows the test accuracy of CIFAR-10 training with DavidNet. The PyTorch implementation (momentum

⁴<https://dawn.cs.stanford.edu/benchmark/CIFAR10/train.html>

Table 6: Untuned LAMB for ImageNet training with RESNET-50 for different batch sizes (90 epochs). We can just use square root LR scaling (Krizhevsky, 2014) and linear-epoch warmup (You et al., 2019). Using this, Goyal et al. (2017) report top-1 accuracy of 76.3% in 90 epochs for the baseline. According to Stanford DAWN Bench, the baseline should achieve 93% top-5 accuracy. LAMB achieves both of them. We can achieve a much better accuracy for 32K if we manually tune the hyperparameters.

Batch Size	512	1K	2K	4K	8K	16K	32K
Learning Rate	$\frac{4}{2^{3.0} \times 100}$	$\frac{4}{2^{2.5} \times 100}$	$\frac{4}{2^{2.0} \times 100}$	$\frac{4}{2^{1.5} \times 100}$	$\frac{4}{2^{1.0} \times 100}$	$\frac{4}{2^{0.5} \times 100}$	$\frac{4}{2^{0.0} \times 100}$
Warmup Epochs	0.3125	0.625	1.25	2.5	5	10	20
Top-5 Accuracy	0.9335	0.9349	0.9353	0.9332	0.9331	0.9322	0.9308
Top-1 Accuracy	0.7696	0.7706	0.7711	0.7692	0.7689	0.7666	0.7642

optimizer) on GPUs was reported on Stanford DAWNBench’s website, which achieves 94.06% in 24 epochs. The Tensorflow implementation (momentum optimizer) on TPU achieves a 93.72% accuracy in 24 epochs⁵. We use the implementation of TensorFlow on TPUs. LAMB optimizer is able to achieve 94.08% test accuracy in 24 epochs, which is better than other adaptive optimizers and momentum. Even on the smaller tasks like MNIST training with LeNet, LAMB is able to achieve a better accuracy than existing solvers (Table 8).

Table 7: CIFAR-10 training with DavidNet (batch size = 512). All of them run 24 epochs and finish the training under 1 minute on 1 TPU. All the adaptive solvers were extensively tuned. The tuning information is reported in the Appendix.

Optimizer	ADAGRAD	ADAM	ADAMW	momentum	LAMB
Test Accuracy	0.9074	0.9225	0.9271	0.9372	0.9408

Table 8: Test Accuracy by MNIST training with LeNet (30 epochs for Batch Size = 1024). The tuning space of learning rate for all the optimizers is {0.0001, 0.001, 0.01, 0.1}. We use the same learning rate warmup and decay schedule for all of them.

Optimizer	Momentum	Addgrad	ADAM	ADAMW	LAMB
Average accuracy over 5 runs	0.9933	0.9928	0.9936	0.9941	0.9945

5 CONCLUSION

Large batch techniques are critical to speeding up deep neural network training. In this paper, we propose the LAMB optimizer, which supports adaptive elementwise updating and layerwise learning rates. Furthermore, LAMB is a general purpose optimizer that works for both small and large batches. We also provided theoretical analysis for the LAMB optimizer, highlighting the cases where it performs better than standard SGD. LAMB achieves better performance than existing optimizers for a wide range of applications. By using LAMB, we are able to scale the batch size of BERT pre-training to 64K without losing accuracy, thereby, reducing the BERT training time from 3 days to around 76 minutes. LAMB is also the first large batch adaptive solver that can achieve state-of-the-art accuracy on ImageNet training with RESNET-50.

6 ACKNOWLEDGEMENT

This paper does not propose LARS optimizer; we only provide its convergence analysis. We want to thank the comments from George Dahl and Jeff Dean. We want to thank Michael Banfield, Dehao Chen, Youlong Cheng, Sameer Kumar, and Zak Stone for TPU Pod support. This technical report is only for the research purpose. The TPU’s speed in this paper should not be considered as Google’s

⁵https://github.com/fenwickslab/dl_tutorials/blob/master/tutorial3_cifar10_davidnet_fix.ipynb

official number. The readers need to check Google's official documents for TPU's speed. The content, views and conclusions presented in this paper do not necessarily reflect the position of Google.

REFERENCES

- Takuya Akiba, Shuji Suzuki, and Keisuke Fukuda. Extremely large minibatch sgd: Training resnet-50 on imagenet in 15 minutes. *arXiv preprint arXiv:1711.04325*, 2017.
- Yoshua Bengio. Practical recommendations for gradient-based training of deep architectures. In *Neural networks: Tricks of the trade*, pp. 437–478. Springer, 2012.
- Jeremy Bernstein, Yu-Xiang Wang, Kamyar Azizzadenesheli, and Anima Anandkumar. signsgd: compressed optimisation for non-convex problems. *CoRR*, abs/1802.04434, 2018.
- Valeriu Codreanu, Damian Podareanu, and Vikram Saletore. Scale out for large minibatch sgd: Residual network training on imagenet-1k with improved accuracy and reduced time to train. *arXiv preprint arXiv:1711.04291*, 2017.
- Jeffrey Dean, Greg Corrado, Rajat Monga, Kai Chen, Matthieu Devin, Mark Mao, Andrew Senior, Paul Tucker, Ke Yang, Quoc V Le, et al. Large scale distributed deep networks. In *Advances in neural information processing systems*, pp. 1223–1231, 2012.
- Aditya Devarakonda, Maxim Naumov, and Michael Garland. Adabatch: Adaptive batch sizes for training deep neural networks. *arXiv preprint arXiv:1712.02029*, 2017.
- Jacob Devlin, Ming-Wei Chang, Kenton Lee, and Kristina Toutanova. Bert: Pre-training of deep bidirectional transformers for language understanding. *arXiv preprint arXiv:1810.04805*, 2018.
- Saeed Ghadimi and Guanghui Lan. Stochastic first- and zeroth-order methods for nonconvex stochastic programming. *SIAM Journal on Optimization*, 23(4):2341–2368, 2013a. doi: 10.1137/120880811.
- Saeed Ghadimi and Guanghui Lan. Stochastic first-and zeroth-order methods for nonconvex stochastic programming. *SIAM Journal on Optimization*, 23(4):2341–2368, 2013b.
- Saeed Ghadimi, Guanghui Lan, and Hongchao Zhang. Mini-batch stochastic approximation methods for nonconvex stochastic composite optimization. *Mathematical Programming*, 155(1-2):267–305, 2014.
- Priya Goyal, Piotr Dollár, Ross Girshick, Pieter Noordhuis, Lukasz Wesolowski, Aapo Kyrola, Andrew Tulloch, Yangqing Jia, and Kaiming He. Accurate, large minibatch sgd: Training imagenet in 1 hour. *arXiv preprint arXiv:1706.02677*, 2017.
- Kaiming He, Xiangyu Zhang, Shaoqing Ren, and Jian Sun. Deep residual learning for image recognition. In *Proceedings of the IEEE conference on computer vision and pattern recognition*, pp. 770–778, 2016.
- Elad Hoffer, Itay Hubara, and Daniel Soudry. Train longer, generalize better: closing the generalization gap in large batch training of neural networks. *arXiv preprint arXiv:1705.08741*, 2017.
- Forrest N Iandola, Matthew W Moskewicz, Khalid Ashraf, and Kurt Keutzer. Firecaffe: near-linear acceleration of deep neural network training on compute clusters. In *Proceedings of the IEEE Conference on Computer Vision and Pattern Recognition*, pp. 2592–2600, 2016.
- Xianyan Jia, Shutao Song, Wei He, Yangzihao Wang, Haidong Rong, Feihu Zhou, Liqiang Xie, Zhenyu Guo, Yuanzhou Yang, Liwei Yu, et al. Highly scalable deep learning training system with mixed-precision: Training imagenet in four minutes. *arXiv preprint arXiv:1807.11205*, 2018.
- Nitish Shirish Keskar, Dheevatsa Mudigere, Jorge Nocedal, Mikhail Smelyanskiy, and Ping Tak Peter Tang. On large-batch training for deep learning: Generalization gap and sharp minima. *arXiv preprint arXiv:1609.04836*, 2016.
- Alex Krizhevsky. One weird trick for parallelizing convolutional neural networks. *arXiv preprint arXiv:1404.5997*, 2014.
- Mu Li. *Scaling Distributed Machine Learning with System and Algorithm Co-design*. PhD thesis, Intel, 2017.

James Martens and Roger Grosse. Optimizing neural networks with kronecker-factored approximate curvature. In *International conference on machine learning*, pp. 2408–2417, 2015.

Hiroaki Mikami, Hisahiro Suganuma, Yoshiki Tanaka, Yuichi Kageyama, et al. Imagenet/resnet-50 training in 224 seconds. *arXiv preprint arXiv:1811.05233*, 2018.

Kazuki Osawa, Yohei Tsuji, Yuichiro Ueno, Akira Naruse, Rio Yokota, and Satoshi Matsuoka. Second-order optimization method for large mini-batch: Training resnet-50 on imagenet in 35 epochs. *arXiv preprint arXiv:1811.12019*, 2018.

Benjamin Recht, Christopher Re, Stephen Wright, and Feng Niu. Hogwild: A lock-free approach to parallelizing stochastic gradient descent. In *Advances in neural information processing systems*, pp. 693–701, 2011.

Christopher J Shallue, Jaehoon Lee, Joe Antognini, Jascha Sohl-Dickstein, Roy Frostig, and George E Dahl. Measuring the effects of data parallelism on neural network training. *arXiv preprint arXiv:1811.03600*, 2018.

Samuel L Smith, Pieter-Jan Kindermans, and Quoc V Le. Don’t decay the learning rate, increase the batch size. *arXiv preprint arXiv:1711.00489*, 2017.

Chris Ying, Sameer Kumar, Dehao Chen, Tao Wang, and Youlong Cheng. Image classification at supercomputer scale. *arXiv preprint arXiv:1811.06992*, 2018.

Yang You, Igor Gitman, and Boris Ginsburg. Scaling sgd batch size to 32k for imagenet training. *arXiv preprint arXiv:1708.03888*, 2017.

Yang You, Zhao Zhang, Cho-Jui Hsieh, James Demmel, and Kurt Keutzer. Imagenet training in minutes. In *Proceedings of the 47th International Conference on Parallel Processing*, pp. 1. ACM, 2018.

Yang You, Jonathan Hseu, Chris Ying, James Demmel, Kurt Keutzer, and Cho-Jui Hsieh. Large-batch training for lstm and beyond. *arXiv preprint arXiv:1901.08256*, 2019.

APPENDIX

A PROOF OF THEOREM 2

Proof. We analyze the convergence of LARS for general minibatch size here. Recall that the update of LARS is the following

$$x_{t+1}^{(i)} = x_t^{(i)} - \eta_t \phi(\|x_t^{(i)}\|) \frac{g_t^{(i)}}{\|g_t^{(i)}\|},$$

for all $i \in [h]$. For simplicity of notation, we reason the

Since the function f is L -smooth, we have the following:

$$\begin{aligned} f(x_{t+1}) &\leq f(x_t) + \langle \nabla_i f(x_t), x_{t+1}^{(i)} - x_t^{(i)} \rangle + \sum_{i=1}^h \frac{L_i}{2} \|x_{t+1}^{(i)} - x_t^{(i)}\|^2 \\ &= f(x_t) - \eta_t \sum_{i=1}^h \sum_{j=1}^{d_i} \phi(\|x_t^{(i)}\|) \times \left([\nabla_i f(x_t)]_j \times \frac{g_{t,j}^{(i)}}{\|g_t^{(i)}\|} \right) + \sum_{i=1}^h \frac{L_i \eta_t^2 \phi^2(\|x_t^{(i)}\|)}{2} \\ &\leq f(x_t) - \eta_t \sum_{i=1}^h \sum_{j=1}^{d_i} \phi(\|x_t^{(i)}\|) \times \left([\nabla_i f(x_t)]_j \times \left(\frac{g_{t,j}^{(i)}}{\|g_t^{(i)}\|} - \frac{[\nabla_i f(x_t)]_j}{\|\nabla_i f(x_t)\|} + \frac{[\nabla_i f(x_t)]_j}{\|\nabla_i f(x_t)\|} \right) \right) + \frac{\eta_t^2 \alpha_u^2}{2} \|L\|_1 \\ &= f(x_t) - \eta_t \sum_{i=1}^h \phi(\|x_t^{(i)}\|) \times \|\nabla_i f(x_t)\| - \eta_t \sum_{i=1}^h \sum_{j=1}^{d_i} \left([\nabla_i f(x_t)]_j \times \left(\frac{g_{t,j}^{(i)}}{\|g_t^{(i)}\|} - \frac{[\nabla_i f(x_t)]_j}{\|\nabla_i f(x_t)\|} \right) \right) + \frac{\eta_t^2 \alpha_u^2}{2} \|L\|_1 \end{aligned} \quad (4)$$

The first inequality follows from the lipschitz continuous nature of the gradient. Let $\Delta_t^{(i)} = g_t^{(i)} - \nabla_i f(x_t)$. Then the above inequality can be rewritten in the following manner:

$$\begin{aligned}
f(x_{t+1}) &\leq f(x_t) - \eta_t \sum_{i=1}^h \phi(\|x_t^{(i)}\|) \|\nabla_i f(x_t)\| \\
&\quad - \eta_t \sum_{i=1}^h \sum_{j=1}^{d_i} \phi(\|x_t^{(i)}\|) \times \left([\nabla_i f(x_t)]_j \times \left(\frac{(\Delta_t^{(i)} + [\nabla_i f(x_t)]_j)}{\|\Delta_t^{(i)} + \nabla_i f(x_t)\|} - \frac{[\nabla_i f(x_t)]_j}{\|\nabla_i f(x_t)\|} \right) \right) + \frac{\eta_t^2 \alpha_u^2}{2} \|L\|_1 \\
&= f(x_t) - \eta_t \sum_{i=1}^h \phi(\|x_t^{(i)}\|) \|\nabla_i f(x_t)\| \\
&\quad - \eta_t \sum_{i=1}^h \phi(\|x_t^{(i)}\|) \times \left(\frac{\langle \Delta_t^{(i)} + \nabla_i f(x_t), \nabla_i f(x_t) \rangle}{\|\Delta_t^{(i)} + \nabla_i f(x_t)\|} - \|\nabla_i f(x_t)\| \right) + \frac{\eta_t^2 \alpha_u^2}{2} \|L\|_1 \\
&= f(x_t) - \eta_t \sum_{i=1}^h \phi(\|x_t^{(i)}\|) \|\nabla_i f(x_t)\| \\
&\quad + \eta_t \sum_{i=1}^h \phi(\|x_t^{(i)}\|) \times \left(\frac{\|\nabla_i f(x_t)\| \|\Delta_t^{(i)} + \nabla_i f(x_t)\| - \langle \Delta_t^{(i)} + \nabla_i f(x_t), \nabla_i f(x_t) \rangle}{\|\Delta_t^{(i)} + \nabla_i f(x_t)\|} \right) + \frac{\eta_t^2 \alpha_u^2}{2} \|L\|_1 \\
&= f(x_t) - \eta_t \sum_{i=1}^h \phi(\|x_t^{(i)}\|) \|\nabla_i f(x_t)\| + \frac{\eta_t^2 \alpha_u^2}{2} \|L\|_1 \\
&\quad + \eta_t \sum_{i=1}^h \phi(\|x_t^{(i)}\|) \times \left(\frac{\|\nabla_i f(x_t)\| \|\Delta_t^{(i)} + \nabla_i f(x_t)\| - \|\Delta_t^{(i)} + \nabla_i f(x_t)\|^2 + \langle \Delta_t^{(i)}, \Delta_t^{(i)} + \nabla_i f(x_t) \rangle}{\|\Delta_t^{(i)} + \nabla_i f(x_t)\|} \right). \tag{5}
\end{aligned}$$

Using Cauchy-Schwarz inequality in the above inequality, we have:

$$\begin{aligned}
f(x_{t+1}) &\leq f(x_t) - \eta_t \sum_{i=1}^h \phi(\|x_t^{(i)}\|) \|\nabla_i f(x_t)\| \\
&\quad + \eta_t \sum_{i=1}^h \phi(\|x_t^{(i)}\|) \times \left(\|\nabla_i f(x_t)\| - \|\Delta_t^{(i)} + \nabla_i f(x_t)\| + \|\Delta_t^{(i)}\| \right) + \frac{\eta_t^2 \alpha_u^2}{2} \|L\|_1 \\
&\leq f(x_t) - \eta_t \sum_{i=1}^h \phi(\|x_t^{(i)}\|) \|\nabla_i f(x_t)\| + 2\eta_t \sum_{i=1}^h \phi(\|x_t^{(i)}\|) \times \|\Delta_t^{(i)}\| + \frac{\eta_t^2 \alpha_u^2}{2} \|L\|_1
\end{aligned}$$

Taking expectation, we obtain the following:

$$\begin{aligned}
\mathbb{E}[f(x_{t+1})] &\leq f(x_t) - \eta_t \sum_{i=1}^h \phi(\|x_t^{(i)}\|) \|\nabla_i f(x_t)\| + 2\eta_t \sum_{i=1}^h \phi(\|x_t^{(i)}\|) \times \mathbb{E}[\|\Delta_t^{(i)}\|] + \frac{\eta_t^2 \alpha_u^2}{2} \|L\|_1 \\
&\leq f(x_t) - \eta_t \alpha_l \sum_{i=1}^h \|\nabla_i f(x_t)\| + 2\eta_t \alpha_u \frac{\|\sigma\|_1}{\sqrt{b}} + \frac{\eta_t^2 \alpha_u^2}{2} \|L\|_1. \tag{6}
\end{aligned}$$

Summing the above inequality for $t = 1$ to T and using telescoping sum, we have the following inequality:

$$\mathbb{E}[f(x_{T+1})] \leq f(x_1) - \eta \alpha_l \sum_{t=1}^T \sum_{i=1}^h \mathbb{E}[\|\nabla_i f(x_t)\|] + 2\eta T \frac{\alpha_u \|\sigma\|_1}{\sqrt{b}} + \frac{\eta^2 \alpha_u^2 T}{2} \|L\|_1.$$

Rearranging the terms of the above inequality, and dividing by $\eta T \alpha_l$, we have:

$$\begin{aligned} \frac{1}{T} \sum_{t=1}^T \sum_{i=1}^h \mathbb{E}[\|\nabla_i f(x_t)\|] &\leq \frac{f(x_1) - \mathbb{E}[f(x_{T+1})]}{T \eta \alpha_l} + \frac{2\alpha_u \|\sigma\|_1}{\sqrt{b} \alpha_l} + \frac{\eta \alpha_u^2}{2\alpha_l} \|L\|_1 \\ &\leq \frac{f(x_1) - f(x^*)}{T \eta \alpha_l} + \frac{2\alpha_u \|\sigma\|_1}{\alpha_l \sqrt{b}} + \frac{\eta \alpha_u^2}{2\alpha_l} \|L\|_1. \end{aligned}$$

□

B PROOF OF THEOREM 3

Proof. We analyze the convergence of LARS for general minibatch size here. Recall that the update of LAMB is the following

$$x_{t+1}^{(i)} = x_t^{(i)} - \eta_t \phi(\|x_t^{(i)}\|) \frac{r_t^{(i)}}{\|r_t^{(i)}\|},$$

for all $i \in [h]$. For simplicity of notation, we reason the

Since the function f is L -smooth, we have the following:

$$\begin{aligned} f(x_{t+1}) &\leq f(x_t) + \langle \nabla_i f(x_t), x_{t+1}^{(i)} - x_t^{(i)} \rangle + \sum_{i=1}^h \frac{L_i}{2} \|x_{t+1}^{(i)} - x_t^{(i)}\|^2 \\ &= f(x_t) - \underbrace{\eta_t \sum_{i=1}^h \sum_{j=1}^{d_i} \phi(\|x_t^{(i)}\|) \times \left([\nabla_i f(x_t)]_j \times \frac{r_{t,j}^{(i)}}{\|r_t^{(i)}\|} \right)}_{T_1} + \sum_{i=1}^h \frac{L_i \alpha_u^2 \eta_t^2}{2} \end{aligned} \quad (7)$$

The above inequality simply follows from the lipschitz continuous nature of the gradient. We bound term T_1 in the following manner:

$$\begin{aligned} T_1 &\leq -\eta_t \sum_{i=1}^h \sum_{j=1}^{d_i} \phi(\|x_t^{(i)}\|) \times \left([\nabla_i f(x_t)]_j \times \frac{r_{t,j}^{(i)}}{\|r_t^{(i)}\|} \right) \\ &\leq -\eta_t \sum_{i=1}^h \sum_{j=1}^{d_i} \sqrt{\frac{1-\beta_2}{G^2 d_i}} \left(\phi(\|x_t^{(i)}\|) \times [\nabla_i f(x_t)]_j \times g_{t,j}^{(i)} \right) \\ &\quad - \eta_t \sum_{i=1}^h \sum_{j=1}^{d_i} \left(\phi(\|x_t^{(i)}\|) \times [\nabla_i f(x_t)]_j \times \frac{r_{t,j}^{(i)}}{\|r_t^{(i)}\|} \right) \mathbb{1}(\text{sign}(\nabla_i f(x_t))_j \neq \text{sign}(r_{t,j}^{(i)})) \end{aligned} \quad (8)$$

This follows from the fact that $\|r_t^{(i)}\| \leq \sqrt{\frac{d_i}{1-\beta_2}}$ and $\sqrt{v_t} \leq G$. If $\beta_2 = 0$, then T_1 can be bounded as follows:

$$\begin{aligned} T_1 &\leq -\eta_t \sum_{i=1}^h \sum_{j=1}^{d_i} \sqrt{\frac{1}{d_i}} \left(\phi(\|x_t^{(i)}\|) \times |[\nabla_i f(x_t)]_j| \right) \\ &\quad - \eta_t \sum_{i=1}^h \sum_{j=1}^{d_i} \left(\phi(\|x_t^{(i)}\|) \times [\nabla_i f(x_t)]_j \times \frac{r_{t,j}^{(i)}}{\|r_t^{(i)}\|} \right) \mathbb{1}(\text{sign}(\nabla_i f(x_t))_j \neq \text{sign}(r_{t,j}^{(i)})) \end{aligned}$$

The rest of the proof for $\beta_2 = 0$ is similar to argument for the case $\beta_2 > 0$, which is shown below. Taking expectation, we have the following:

$$\begin{aligned}
\mathbb{E}[T_1] &\leq -\eta_t \sum_{i=1}^h \sum_{j=1}^{d_i} \sqrt{\frac{1-\beta_2}{G^2 d_i}} \mathbb{E} \left[\phi(\|x_t^{(i)}\|) \times \left([\nabla_i f(x_t)]_j \times g_{t,j}^{(i)} \right) \right] \\
&\quad - \eta_t \sum_{i=1}^h \sum_{j=1}^{d_i} \mathbb{E} \left[\phi(\|x_t^{(i)}\|) \times \left([\nabla_i f(x_t)]_j \times \frac{r_{t,j}^{(i)}}{\|r_t^{(i)}\|} \right) \mathbf{1}(\text{sign}(\nabla_i f(x_t))_j \neq \text{sign}(g_{t,j}^{(i)})) \right] \\
&\leq -\eta_t \sum_{i=1}^h \sum_{j=1}^{d_i} \sqrt{\frac{1-\beta_2}{G^2 d_i}} \mathbb{E} \left[\left(\phi(\|x_t^{(i)}\|) \times [\nabla_i f(x_t)]_j \times g_{t,j}^{(i)} \right) \right] \\
&\quad + \eta_t \sum_{i=1}^h \sum_{j=1}^{d_i} \mathbb{E} \left[\alpha_u |\nabla_i f(x_t)_j| \mathbf{1}(\text{sign}(\nabla_i f(x_t))_j \neq \text{sign}(g_{t,j}^{(i)})) \right] \\
&\leq -\eta_t \sum_{i=1}^h \sum_{j=1}^{d_i} \sqrt{\frac{1-\beta_2}{G^2 d_i}} \mathbb{E} \left[\phi(\|x_t^{(i)}\|) \times \left([\nabla_i f(x_t)]_j \times g_{t,j}^{(i)} \right) \right] \\
&\quad - \eta_t \sum_{i=1}^h \sum_{j=1}^{d_i} \alpha_u |\nabla_i f(x_t)_j| \mathbb{P}(\text{sign}(\nabla_i f(x_t))_j \neq \text{sign}(g_{t,j}^{(i)}))
\end{aligned} \tag{9}$$

Using the bound on the probability that the signs differ, we get:

$$\mathbb{E}[T_1] \leq -\eta_t \alpha_l \sqrt{\frac{h(1-\beta_2)}{G^2 d}} \|\nabla f(x_t)\|^2 + \eta_t \alpha_u \sum_{i=1}^h \sum_{j=1}^{d_i} \frac{\sigma_{i,j}}{\sqrt{b}}.$$

Substituting the above bound on T_1 in equation 7, we have the following bound:

$$\mathbb{E}[f(x_{t+1})] \leq f(x_t) - \eta_t \alpha_l \sqrt{\frac{h(1-\beta_2)}{G^2 d}} \|\nabla f(x_t)\|^2 + \eta_t \alpha_u \frac{\|\tilde{\sigma}\|_1}{\sqrt{b}} + \frac{\eta_t^2 \alpha_u^2 \|L\|_1}{2} \tag{10}$$

Summing the above inequality for $t = 1$ to T and using telescoping sum, we have the following inequality:

$$\mathbb{E}[f(x_{T+1})] \leq f(x_1) - \eta_t \alpha_l \sqrt{\frac{h(1-\beta_2)}{G^2 d}} \sum_{t=1}^T \mathbb{E}[\|\nabla f(x_t)\|^2] + \eta T \alpha_u \frac{\|\tilde{\sigma}\|_1}{\sqrt{b}} + \frac{\eta^2 \alpha_u^2 T}{2} \|L\|_1.$$

Rearranging the terms of the above inequality, and dividing by $\eta T \alpha_l$, we have:

$$\begin{aligned}
\sqrt{\frac{h(1-\beta_2)}{G^2 d}} \frac{1}{T} \sum_{t=1}^T \mathbb{E}[\|\nabla f(x_t)\|^2] &\leq \frac{f(x_1) - \mathbb{E}[f(x_{T+1})]}{T \eta \alpha_l} + \frac{\alpha_u \|\tilde{\sigma}\|_1}{\alpha_l \sqrt{b}} + \frac{\eta}{2} \|L\|_1 \\
&\leq \frac{f(x_1) - f(x^*)}{T \eta \alpha_l} + \frac{\alpha_u \|\tilde{\sigma}\|_1}{\alpha_l \sqrt{b}} + \frac{\eta \alpha_u^2}{2 \alpha_l} \|L\|_1.
\end{aligned}$$

□

C COMPARISON OF CONVERGENCE RATES OF LARS AND SGD

Inspired by the comparison used by (Bernstein et al., 2018) for comparing SIGN SGD with SGD, we define the following quantities:

$$\begin{aligned}
\left(\sum_{i=1}^h \|\nabla_i f(x_t)\| \right)^2 &= \frac{\psi(\nabla f(x_t)) d \|\nabla f(x_t)\|^2}{h} \geq \frac{\psi_g d \|\nabla f(x_t)\|^2}{h} \\
\|L\|_1^2 &\leq \frac{\psi_L d^2 \|L\|_\infty^2}{h^2} \\
\|\sigma\|_1^2 &= \frac{\psi_\sigma d \|\sigma\|^2}{h}.
\end{aligned}$$

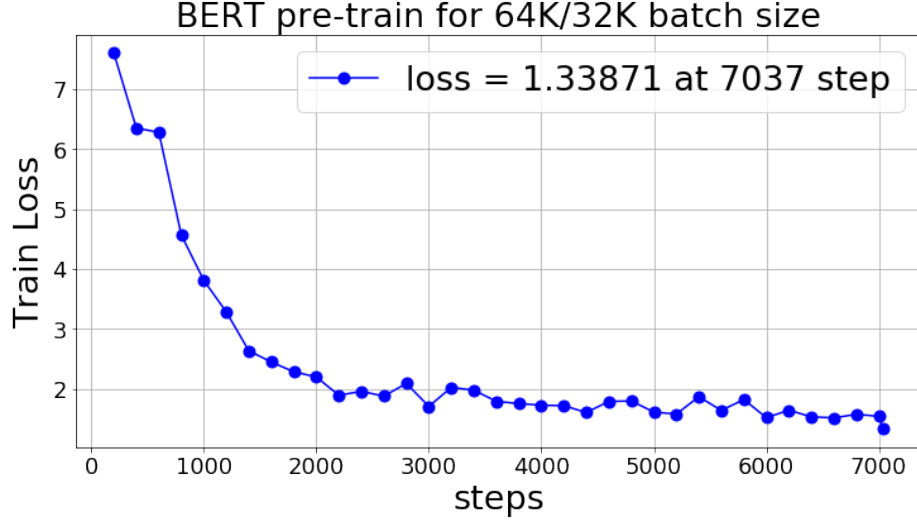


Figure 3: This figure shows the training loss curve of LAMB optimizer. Our experiments show that training loss values are not necessarily meaningful. We just want to use this figure to show that LAMB can make the training converge smoothly.

Then LARS convergence rate can be written in the following manner:

$$(\mathbb{E}[\|\nabla f(x_a)\|])^2 \leq O\left(\frac{(f(x_1) - f(x^*))L_\infty}{T} \frac{\psi_L}{\psi_g^2} + \frac{\|\sigma\|^2}{T} \frac{\psi_\sigma^2}{\psi_g^2}\right).$$

If $\psi_L \ll \psi_g^2$ and $\psi_\sigma \ll \psi_g^2$ then LARS (i.e., gradient is more denser than curvature or stochasticity), we gain over SGD. Otherwise, SGD’s upper bound on convergence rate is better.

D ADDITIONAL RESULTS

β_1 is used for decaying the running average of the gradient. β_2 is used for decaying the running average of the square of gradient. The default setting for other parameters: weight decay rate $\lambda=0.01$, $\beta_1=0.9$, $\beta_2=0.999$, $\epsilon=1e-6$.

Based on our experience, learning rate is the most important hyper-parameter that affects the learning efficiency and final accuracy. Bengio (Bengio, 2012) suggests that it is often the single most important hyper-parameter and that it always should be tuned.

In our experiments, we found that the validation loss is not reliable. A lower validation loss does not necessarily lead to a higher validation accuracy (Figure 4). Thus, we use the test/val accuracy or F1 score on dev set to evaluate the optimizers.

D.0.1 BERT

The training loss curve of BERT pre-training with LAMB is shown in Figure 3. Our experiments show that training loss values are not necessarily meaningful. We often observe a lower training loss leads to a worse testing accuracy. We just want to use this figure to show that LAMB can make the training converge smoothly at the batch size of 64K.

Figures 5 - 10 show the LAMB trust ratio at different iterations for ImageNet training with ResNet-50. From these figures we can see that these ratios are very different from each other for different layers. LAMB uses the trust ratio to help the slow learners to train faster.

D.0.2 CIFAR-10

We make sure all the solvers are carefully tuned. The learning rate tuning space of Adam, AdamW, Adagrad and LAMB is $\{0.0001, 0.0002, 0.0004, 0.0006, 0.0008, 0.001, 0.002, 0.004, 0.006, 0.008,$

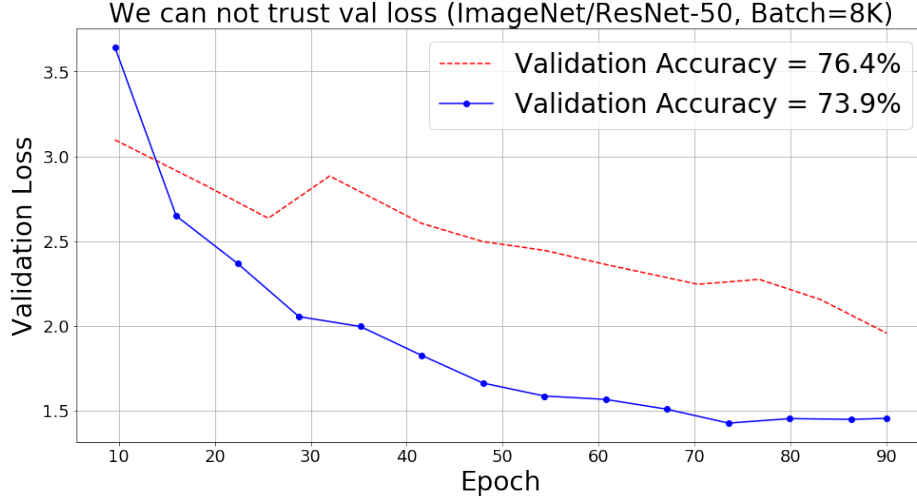


Figure 4: Our experiments show that even the validation loss is not reliable in the large-scale training. A lower validation loss may lead to a worse accuracy.

0.01, 0.02, 0.04, 0.06, 0.08, 0.1, 0.2, 0.4, 0.6, 0.8, 1, 2, 4, 6, 8, 10, 15, 20, 25, 30, 35, 40, 45, 50}. The momentum optimizer was tuned by the baseline implementer. The weight decay term of AdamW was tuned by {0.0001, 0.001, 0.01, 0.1, 1.0}.

D.0.3 IMAGENET

[Goyal et al. \(2017\)](#) suggested proper learning rate warmup and learning rate decay may help improve the ImageNet classification accuracy. We included these techniques in Adam/AdamW/AdaGrad tuning. Specifically, we use the learning rate recipe of ([Goyal et al., 2017](#)): (1) 5-epoch warmup to stabilize the initial stage; and (2) multiply the learning rate by 0.1 at 30th, 60th, and 80th epoch. The target accuracy is around 0.763 ([Goyal et al., 2017](#)). These techniques help to improve the accuracy of Adam to around 73%. However, even with these techniques, Adam/AdamW/AdaGrad still can not achieve the target validation accuracy.

D.1 BASELINE TUNING DETAILS FOR IMAGENET TRAINING WITH RESNET-50

To make sure our baseline is solid, we carefully tuned the hyper-parameters. Table 9 shows the tuning information of standard Adagrad. Table 10 shows the tuning information of adding the learning rate scheme of [Goyal et al. \(2017\)](#) to standard Adagrad. Table 11 shows the tuning information of standard Adam. Table shows the tuning information of adding the learning rate scheme of [Goyal et al. \(2017\)](#) to standard Adam. It is tricky to tune the AdamW optimizer since both the L2 regularization and weight decay have the effect on the performance. Thus we have four tuning sets.

The first tuning set is based on AdamW with default L2 regularization. We tune the learning rate and weight decay. The tuning information is in Figures 13, 14, 15, and 16.

The second tuning set is based on AdamW with disabled L2 regularization. We tune the learning rate and weight decay. The tuning information is in Figures 17, 18, 19, and 20.

Then we add the learning rate scheme of [Goyal et al. \(2017\)](#) to AdamW and refer to it as AdamW+.

The third tuning set is based on AdamW+ with default L2 regularization. We tune the learning rate and weight decay. The tuning information is Figure 21 and 22.

The fourth tuning set is based on AdamW+ with disabled L2 regularization. We tune the learning rate and weight decay. The tuning information is in Figures 23, 24, 25.

Based on our comprehensive tuning results, we conclude the existing adaptive solvers do not perform well on ImageNet training or at least it is hard to tune them.

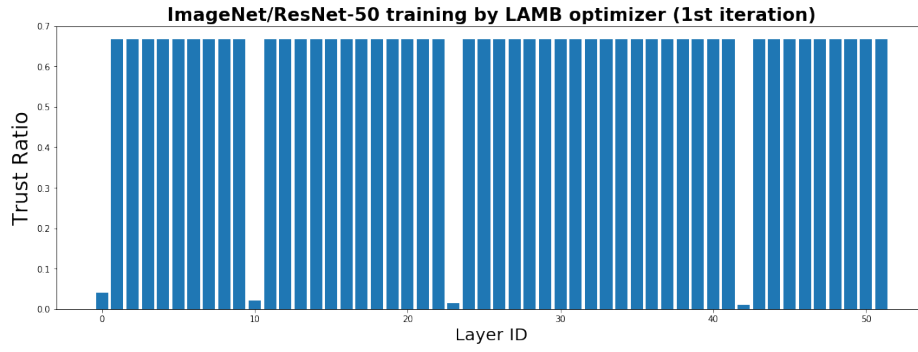


Figure 5: The LAMB trust ratio.

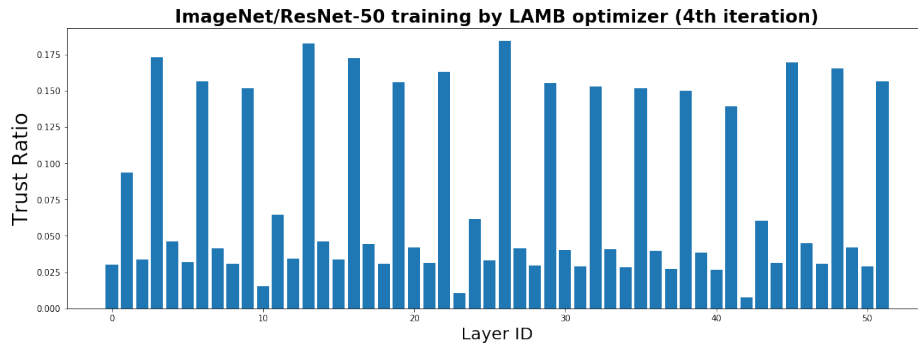


Figure 6: The LAMB trust ratio.

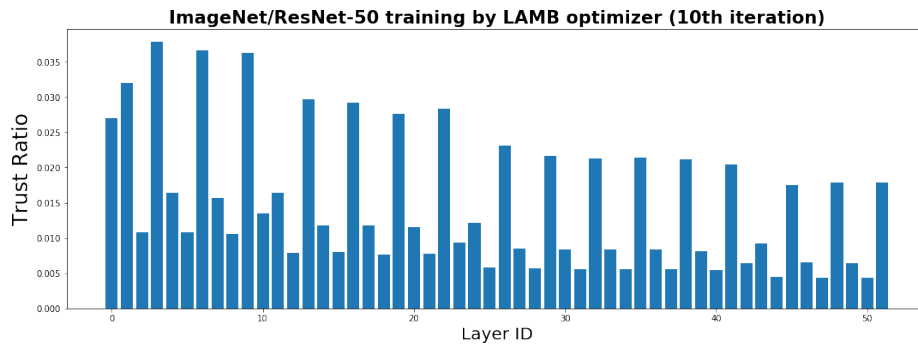


Figure 7: The LAMB trust ratio.

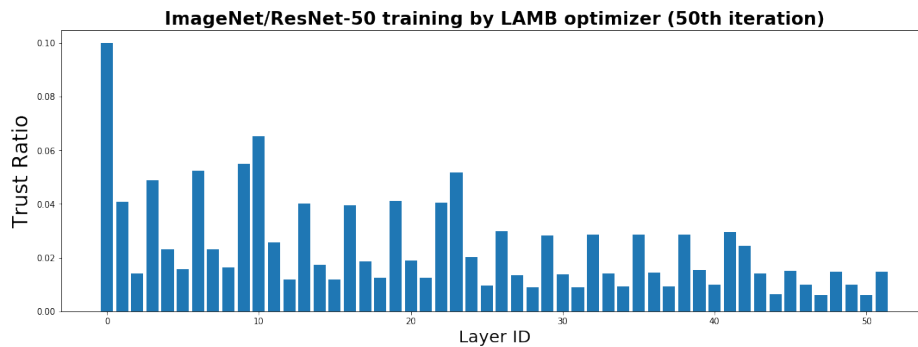


Figure 8: The LAMB trust ratio.

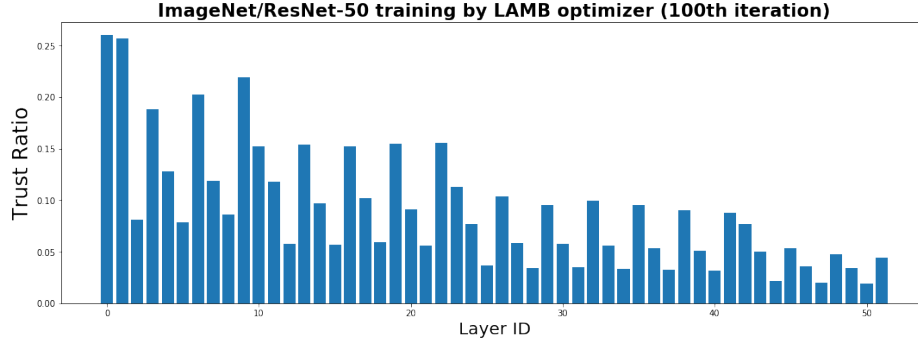


Figure 9: The LAMB trust ratio.

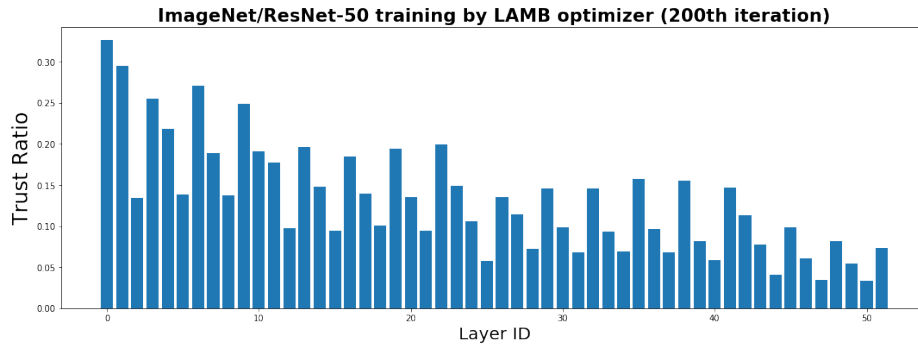


Figure 10: The LAMB trust ratio.

Table 9: The accuracy information of tuning default AdaGrad optimizer for ImageNet training with ResNet-50 (batch size = 16384, 90 epochs, 7038 iterations).

Learning Rate	Top-1 Validation Accuracy
0.0001	0.0026855469
0.001	0.015563965
0.002	0.022684732
0.004	0.030924479
0.008	0.04486084
0.010	0.054158527
0.020	0.0758667
0.040	0.1262614
0.080	0.24037679
0.100	0.27357993
0.200	0.458313
0.400	0.553833
0.800	0.54103595
1.000	0.5489095
2.000	0.47680664
4.000	0.5295207
6.000	0.36950684
8.000	0.31081137
10.00	0.30670166
12.00	0.3091024
14.00	0.3227946
16.00	0.0063680015
18.00	0.11287435
20.00	0.21602376
30.00	0.08315023
40.00	0.0132039385
50.00	0.0009969076

Table 10: The accuracy information of tuning AdaGrad optimizer for ImageNet training with ResNet-50 (batch size = 16384, 90 epochs, 7038 iterations). We use the learning rate recipe of (Goyal et al., 2017): (1) 5-epoch warmup to stabilize the initial stage; and (2) multiply the learning rate by 0.1 at 30th, 60th, and 80th epoch. The target accuracy is around 0.763 (Goyal et al., 2017).

Learning Rate	Top-1 Validation Accuracy
0.0001	0.0011189779
0.001	0.00793457
0.002	0.012573242
0.004	0.019022623
0.008	0.027079264
0.010	0.029012045
0.020	0.0421346
0.040	0.06618246
0.080	0.10970052
0.100	0.13429768
0.200	0.26550293
0.400	0.41918945
0.800	0.5519816
1.000	0.58614093
2.000	0.67252606
4.000	0.70306396
6.000	0.709493
8.000	0.7137858
10.00	0.71797687
12.00	0.7187703
14.00	0.72007245
16.00	0.7194214
18.00	0.7149251
20.00	0.71293133
30.00	0.70458984
40.00	0.69085693
50.00	0.67976886

Table 11: The accuracy information of tuning default Adam optimizer for ImageNet training with ResNet-50 (batch size = 16384, 90 epochs, 7038 iterations). The target accuracy is around 0.763 (Goyal et al., 2017).

Learning Rate	Top-1 Validation Accuracy
0.0001	0.5521
0.0002	0.6089
0.0004	0.6432
0.0006	0.6465
0.0008	0.6479
0.001	0.6604
0.002	0.6408
0.004	0.5687
0.006	0.5165
0.008	0.4812
0.010	0.3673

Table 12: The accuracy information of tuning Adam optimizer for ImageNet training with ResNet-50 (batch size = 16384, 90 epochs, 7038 iterations). We use the learning rate recipe of (Goyal et al., 2017): (1) 5-epoch warmup to stabilize the initial stage; and (2) multiply the learning rate by 0.1 at 30th, 60th, and 80th epoch. The target accuracy is around 0.763 (Goyal et al., 2017).

Learning Rate	Top-1 Validation Accuracy
0.0001	0.410319
0.0002	0.55263263
0.0004	0.6455485
0.0006	0.6774495
0.0008	0.6996867
0.001	0.71010333
0.002	0.73476154
0.004	0.73286945
0.006	0.72648114
0.008	0.72214764
0.010	0.71466064
0.012	0.7081502
0.014	0.6993001
0.016	0.69108075
0.020	0.67997235
0.040	0.58658856
0.060	0.51090497
0.080	0.45174155
0.100	0.40297446

Table 13: The accuracy information of tuning default AdamW optimizer for ImageNet training with ResNet-50 (batch size = 16384, 90 epochs, 7038 iterations). The target accuracy is around 0.763 (Goyal et al., 2017).

learning rate	weight decay	L2 regularization	Top-1 Validation Accuracy
0.0001	0.00001	default (0.01)	0.53312176
0.0002	0.00001	default (0.01)	0.5542806
0.0004	0.00001	default (0.01)	0.48769125
0.0006	0.00001	default (0.01)	0.46317545
0.0008	0.00001	default (0.01)	0.40903726
0.001	0.00001	default (0.01)	0.42401123
0.002	0.00001	default (0.01)	0.33870444
0.004	0.00001	default (0.01)	0.12339274
0.006	0.00001	default (0.01)	0.122924805
0.008	0.00001	default (0.01)	0.08099365
0.010	0.00001	default (0.01)	0.016764322
0.012	0.00001	default (0.01)	0.032714844
0.014	0.00001	default (0.01)	0.018147787
0.016	0.00001	default (0.01)	0.0066731772
0.018	0.00001	default (0.01)	0.010294597
0.020	0.00001	default (0.01)	0.008260091
0.025	0.00001	default (0.01)	0.008870442
0.030	0.00001	default (0.01)	0.0064493814
0.040	0.00001	default (0.01)	0.0018107096
0.050	0.00001	default (0.01)	0.003540039

Table 14: The accuracy information of tuning default AdamW optimizer for ImageNet training with ResNet-50 (batch size = 16384, 90 epochs, 7038 iterations). The target accuracy is around 0.763 (Goyal et al., 2017).

learning rate	weight decay	L2 regularization	Top-1 Validation Accuracy
0.0001	0.0001	default (0.01)	0.55489093
0.0002	0.0001	default (0.01)	0.56514484
0.0004	0.0001	default (0.01)	0.4986979
0.0006	0.0001	default (0.01)	0.47595215
0.0008	0.0001	default (0.01)	0.44685873
0.001	0.0001	default (0.01)	0.41029868
0.002	0.0001	default (0.01)	0.2808024
0.004	0.0001	default (0.01)	0.08111572
0.006	0.0001	default (0.01)	0.068115234
0.008	0.0001	default (0.01)	0.057922363
0.010	0.0001	default (0.01)	0.05222575
0.012	0.0001	default (0.01)	0.017313639
0.014	0.0001	default (0.01)	0.029785156
0.016	0.0001	default (0.01)	0.016540527
0.018	0.0001	default (0.01)	0.00575765
0.020	0.0001	default (0.01)	0.0102335615
0.025	0.0001	default (0.01)	0.0060831704
0.030	0.0001	default (0.01)	0.0036417644
0.040	0.0001	default (0.01)	0.0010782877
0.050	0.0001	default (0.01)	0.0037638347

Table 15: The accuracy information of tuning default AdamW optimizer for ImageNet training with ResNet-50 (batch size = 16384, 90 epochs, 7038 iterations). The target accuracy is around 0.763 (Goyal et al., 2017).

learning rate	weight decay	L2 regularization	Top-1 Validation Accuracy
0.0001	0.001	default (0.01)	0.21142578
0.0002	0.001	default (0.01)	0.4289144
0.0004	0.001	default (0.01)	0.13537598
0.0006	0.001	default (0.01)	0.33803305
0.0008	0.001	default (0.01)	0.32611084
0.001	0.001	default (0.01)	0.22194417
0.002	0.001	default (0.01)	0.1833903
0.004	0.001	default (0.01)	0.08256022
0.006	0.001	default (0.01)	0.020507812
0.008	0.001	default (0.01)	0.018269857
0.010	0.001	default (0.01)	0.007507324
0.012	0.001	default (0.01)	0.020080566
0.014	0.001	default (0.01)	0.010762532
0.016	0.001	default (0.01)	0.0021362305
0.018	0.001	default (0.01)	0.007954915
0.020	0.001	default (0.01)	0.005859375
0.025	0.001	default (0.01)	0.009724935
0.030	0.001	default (0.01)	0.0019124349
0.040	0.001	default (0.01)	0.00390625
0.050	0.001	default (0.01)	0.0009969076

Table 16: The accuracy information of tuning default AdamW optimizer for ImageNet training with ResNet-50 (batch size = 16384, 90 epochs, 7038 iterations). The target accuracy is around 0.763 (Goyal et al., 2017).

learning rate	weight decay	L2 regularization	Top-1 Validation Accuracy
0.0001	0.01	default (0.01)	0.0009765625
0.0002	0.01	default (0.01)	0.0009969076
0.0004	0.01	default (0.01)	0.0010172526
0.0006	0.01	default (0.01)	0.0009358724
0.0008	0.01	default (0.01)	0.0022379558
0.001	0.01	default (0.01)	0.001566569
0.002	0.01	default (0.01)	0.009480794
0.004	0.01	default (0.01)	0.0033569336
0.006	0.01	default (0.01)	0.0029907227
0.008	0.01	default (0.01)	0.0018513998
0.010	0.01	default (0.01)	0.009134929
0.012	0.01	default (0.01)	0.0022176106
0.014	0.01	default (0.01)	0.0040690103
0.016	0.01	default (0.01)	0.0017293295
0.018	0.01	default (0.01)	0.00061035156
0.020	0.01	default (0.01)	0.0022379558
0.025	0.01	default (0.01)	0.0017089844
0.030	0.01	default (0.01)	0.0014241537
0.040	0.01	default (0.01)	0.0020345051
0.050	0.01	default (0.01)	0.0012817383

Table 17: The accuracy information of tuning default AdamW optimizer for ImageNet training with ResNet-50 (batch size = 16384, 90 epochs, 7038 iterations). The target accuracy is around 0.763 (Goyal et al., 2017).

learning rate	weight decay	L2 regularization	Top-1 Validation Accuracy
0.0001	0.00001	disable	0.48917642
0.0002	0.00001	disable	0.58152264
0.0004	0.00001	disable	0.63460284
0.0006	0.00001	disable	0.64849854
0.0008	0.00001	disable	0.6598918
0.001	0.00001	disable	0.6662801
0.002	0.00001	disable	0.67266846
0.004	0.00001	disable	0.6692708
0.006	0.00001	disable	0.6573079
0.008	0.00001	disable	0.6639404
0.010	0.00001	disable	0.65230304
0.012	0.00001	disable	0.6505534
0.014	0.00001	disable	0.64990234
0.016	0.00001	disable	0.65323895
0.018	0.00001	disable	0.67026776
0.020	0.00001	disable	0.66086835
0.025	0.00001	disable	0.65425617
0.030	0.00001	disable	0.6476237
0.040	0.00001	disable	0.55478925
0.050	0.00001	disable	0.61869305

Table 18: The accuracy information of tuning default AdamW optimizer for ImageNet training with ResNet-50 (batch size = 16384, 90 epochs, 7038 iterations). The target accuracy is around 0.763 (Goyal et al., 2017).

learning rate	weight decay	L2 regularization	Top-1 Validation Accuracy
0.0001	0.0001	disable	0.5033366
0.0002	0.0001	disable	0.5949707
0.0004	0.0001	disable	0.62561035
0.0006	0.0001	disable	0.6545207
0.0008	0.0001	disable	0.66326904
0.001	0.0001	disable	0.6677043
0.002	0.0001	disable	0.67244464
0.004	0.0001	disable	0.6702881
0.006	0.0001	disable	0.66033936
0.008	0.0001	disable	0.66426593
0.010	0.0001	disable	0.66151935
0.012	0.0001	disable	0.6545817
0.014	0.0001	disable	0.65509033
0.016	0.0001	disable	0.6529338
0.018	0.0001	disable	0.65651447
0.020	0.0001	disable	0.65334064
0.025	0.0001	disable	0.655009
0.030	0.0001	disable	0.64552814
0.040	0.0001	disable	0.6425374
0.050	0.0001	disable	0.5988159

Table 19: The accuracy information of tuning default AdamW optimizer for ImageNet training with ResNet-50 (batch size = 16384, 90 epochs, 7038 iterations). The target accuracy is around 0.763 (Goyal et al., 2017).

learning rate	weight decay	L2 regularization	Top-1 Validation Accuracy
0.0001	0.001	disable	0.4611206
0.0002	0.001	disable	0.0076293945
0.0004	0.001	disable	0.29233804
0.0006	0.001	disable	0.57295734
0.0008	0.001	disable	0.5574748
0.001	0.001	disable	0.5988566
0.002	0.001	disable	0.586263
0.004	0.001	disable	0.62076825
0.006	0.001	disable	0.61503094
0.008	0.001	disable	0.4697876
0.010	0.001	disable	0.619751
0.012	0.001	disable	0.54243976
0.014	0.001	disable	0.5429077
0.016	0.001	disable	0.55281574
0.018	0.001	disable	0.5819295
0.020	0.001	disable	0.5938924
0.025	0.001	disable	0.541097
0.030	0.001	disable	0.45890298
0.040	0.001	disable	0.56193036
0.050	0.001	disable	0.5279134

Table 20: The accuracy information of tuning default AdamW optimizer for ImageNet training with ResNet-50 (batch size = 16384, 90 epochs, 7038 iterations). The target accuracy is around 0.763 (Goyal et al., 2017).

learning rate	weight decay	L2 regularization	Top-1 Validation Accuracy
0.0001	0.01	disable	0.0009969076
0.0002	0.01	disable	0.0008951823
0.0004	0.01	disable	0.00095621747
0.0006	0.01	disable	0.0012817383
0.0008	0.01	disable	0.016886393
0.001	0.01	disable	0.038146973
0.002	0.01	disable	0.0015258789
0.004	0.01	disable	0.0014241537
0.006	0.01	disable	0.081441246
0.008	0.01	disable	0.028116861
0.010	0.01	disable	0.011820476
0.012	0.01	disable	0.08138021
0.014	0.01	disable	0.010111491
0.016	0.01	disable	0.0041910806
0.018	0.01	disable	0.0038248699
0.020	0.01	disable	0.002746582
0.025	0.01	disable	0.011555989
0.030	0.01	disable	0.0065104165
0.040	0.01	disable	0.016438803
0.050	0.01	disable	0.007710775

Table 21: The accuracy information of tuning AdamW optimizer for ImageNet training with ResNet-50 (batch size = 16384, 90 epochs, 7038 iterations). We use the learning rate recipe of (Goyal et al., 2017): (1) 5-epoch warmup to stabilize the initial stage; and (2) multiply the learning rate by 0.1 at 30th, 60th, and 80th epoch. The target accuracy is around 0.763 (Goyal et al., 2017).

learning rate	weight decay	L2 regularization	Top-1 Validation Accuracy
0.0001	0.01	default (0.01)	0.0009969076
0.0002	0.01	default (0.01)	0.0009969076
0.0004	0.01	default (0.01)	0.0009969076
0.0006	0.01	default (0.01)	0.0009358724
0.0008	0.01	default (0.01)	0.0009969076
0.001	0.01	default (0.01)	0.0009765625
0.002	0.01	default (0.01)	0.0010172526
0.004	0.01	default (0.01)	0.0010172526
0.006	0.01	default (0.01)	0.0010172526
0.008	0.01	default (0.01)	0.0010172526
0.0001	0.001	default (0.01)	0.0010172526
0.0002	0.001	default (0.01)	0.0010172526
0.0004	0.001	default (0.01)	0.0010172526
0.0006	0.001	default (0.01)	0.0009969076
0.0008	0.001	default (0.01)	0.0010172526
0.001	0.001	default (0.01)	0.0010172526
0.002	0.001	default (0.01)	0.0010172526
0.004	0.001	default (0.01)	0.0038452148
0.006	0.001	default (0.01)	0.011881511
0.008	0.001	default (0.01)	0.0061442056

Table 22: The accuracy information of tuning AdamW optimizer for ImageNet training with ResNet-50 (batch size = 16384, 90 epochs, 7038 iterations). We use the learning rate recipe of (Goyal et al., 2017): (1) 5-epoch warmup to stabilize the initial stage; and (2) multiply the learning rate by 0.1 at 30th, 60th, and 80th epoch. The target accuracy is around 0.763 (Goyal et al., 2017).

learning rate	weight decay	L2 regularization	Top-1 Validation Accuracy
0.0001	0.0001	default (0.01)	0.3665975
0.0002	0.0001	default (0.01)	0.5315755
0.0004	0.0001	default (0.01)	0.6369222
0.0006	0.0001	default (0.01)	0.6760457
0.0008	0.0001	default (0.01)	0.69557697
0.001	0.0001	default (0.01)	0.7076009
0.002	0.0001	default (0.01)	0.73065186
0.004	0.0001	default (0.01)	0.72806805
0.006	0.0001	default (0.01)	0.72161865
0.008	0.0001	default (0.01)	0.71816
0.0001	0.00001	default (0.01)	0.49804688
0.0002	0.00001	default (0.01)	0.6287028
0.0004	0.00001	default (0.01)	0.6773885
0.0006	0.00001	default (0.01)	0.67348224
0.0008	0.00001	default (0.01)	0.6622111
0.001	0.00001	default (0.01)	0.6468709
0.002	0.00001	default (0.01)	0.5846761
0.004	0.00001	default (0.01)	0.4868978
0.006	0.00001	default (0.01)	0.34969077
0.008	0.00001	default (0.01)	0.31193033

Table 23: The accuracy information of tuning AdamW optimizer for ImageNet training with ResNet-50 (batch size = 16384, 90 epochs, 7038 iterations). We use the learning rate recipe of (Goyal et al., 2017): (1) 5-epoch warmup to stabilize the initial stage; and (2) multiply the learning rate by 0.1 at 30th, 60th, and 80th epoch. The target accuracy is around 0.763 (Goyal et al., 2017).

learning rate	weight decay	L2 regularization	Top-1 Validation Accuracy
0.0001	0.01	disable	0.0010172526
0.0002	0.01	disable	0.0009765625
0.0004	0.01	disable	0.0010172526
0.0006	0.01	disable	0.0009969076
0.0008	0.01	disable	0.0010172526
0.001	0.01	disable	0.0009765625
0.002	0.01	disable	0.0009969076
0.004	0.01	disable	0.0009969076
0.006	0.01	disable	0.0009765625
0.008	0.01	disable	0.0010172526
0.0001	0.001	disable	0.0009765625
0.0002	0.001	disable	0.0010172526
0.0004	0.001	disable	0.0010172526
0.0006	0.001	disable	0.0010172526
0.0008	0.001	disable	0.0010172526
0.001	0.001	disable	0.0009969076
0.002	0.001	disable	0.0010579427
0.004	0.001	disable	0.0016886393
0.006	0.001	disable	0.019714355
0.008	0.001	disable	0.1329956

Table 24: The accuracy information of tuning AdamW optimizer for ImageNet training with ResNet-50 (batch size = 16384, 90 epochs, 7038 iterations). We use the learning rate recipe of (Goyal et al., 2017): (1) 5-epoch warmup to stabilize the initial stage; and (2) multiply the learning rate by 0.1 at 30th, 60th, and 80th epoch. The target accuracy is around 0.763 (Goyal et al., 2017).

learning rate	weight decay	L2 regularization	Top-1 Validation Accuracy
0.0001	0.0001	disable	0.28515625
0.0002	0.0001	disable	0.44055176
0.0004	0.0001	disable	0.56815594
0.0006	0.0001	disable	0.6234741
0.0008	0.0001	disable	0.6530762
0.001	0.0001	disable	0.6695964
0.002	0.0001	disable	0.70048016
0.004	0.0001	disable	0.71698
0.006	0.0001	disable	0.72021484
0.008	0.0001	disable	0.7223918
0.010	0.0001	disable	0.72017413
0.012	0.0001	disable	0.72058105
0.014	0.0001	disable	0.7188924
0.016	0.0001	disable	0.71695966
0.018	0.0001	disable	0.7154134
0.020	0.0001	disable	0.71358234
0.025	0.0001	disable	0.7145386
0.030	0.0001	disable	0.7114258
0.040	0.0001	disable	0.7066447
0.050	0.0001	disable	0.70284015

Table 25: The accuracy information of tuning AdamW optimizer for ImageNet training with ResNet-50 (batch size = 16384, 90 epochs, 7038 iterations). We use the learning rate recipe of (Goyal et al., 2017): (1) 5-epoch warmup to stabilize the initial stage; and (2) multiply the learning rate by 0.1 at 30th, 60th, and 80th epoch. The target accuracy is around 0.763 (Goyal et al., 2017).

learning rate	weight decay	L2 regularization	Top-1 Validation Accuracy
0.0001	0.00001	disable	0.31247965
0.0002	0.00001	disable	0.4534912
0.0004	0.00001	disable	0.57765704
0.0006	0.00001	disable	0.6277669
0.0008	0.00001	disable	0.65321857
0.001	0.00001	disable	0.6682129
0.002	0.00001	disable	0.69938153
0.004	0.00001	disable	0.7095947
0.006	0.00001	disable	0.710612
0.008	0.00001	disable	0.70857745
0.010	0.00001	disable	0.7094116
0.012	0.00001	disable	0.70717365
0.014	0.00001	disable	0.7109375
0.016	0.00001	disable	0.7058309
0.018	0.00001	disable	0.7052409
0.020	0.00001	disable	0.7064412
0.025	0.00001	disable	0.7035319
0.030	0.00001	disable	0.6994629
0.040	0.00001	disable	0.6972656
0.050	0.00001	disable	0.6971232